



Article

Binding to Iron Quercetin Complexes Increases the Antioxidant Capacity of the Major Birch Pollen Allergen Bet v 1 and Reduces Its Allergenicity

Andreas Regner¹, Nathalie Szepannek¹, Markus Wiederstein² , Aila Fakhimahmadi^{1,3}, Luis F. Paciosis⁴ , Bart R. Blokhuis⁵ , Frank A. Redegeld⁵ , Gerlinde Hofstetter¹, Zdenek Dvorak⁶ , Erika Jensen-Jarolim^{1,3} , Karin Hufnagl^{1,3} and Franziska Roth-Walter^{1,3,*}

- ¹ Comparative Medicine, The Interuniversity Messerli Research Institute of the University of Veterinary Medicine Vienna, Medical University Vienna and University of Vienna, 1210 Vienna, Austria
 - ² Department of Biosciences, University of Salzburg, 5020 Salzburg, Austria
 - ³ Center of Pathophysiology, Infectiology and Immunology, Institute of Pathophysiology and Allergy Research, Medical University of Vienna, 1090 Vienna, Austria
 - ⁴ Center for Plant Biotechnology and Genomics, Biotechnology Department, ETSIAAB, CBGP (UPM-INIA), Universidad Politécnica de Madrid, 28040 Madrid, Spain
 - ⁵ Division of Pharmacology, Utrecht Institute for Pharmaceutical Sciences, Faculty of Science, Utrecht University, 3584 CG Utrecht, The Netherlands
 - ⁶ Department of Cell Biology and Genetics, Faculty of Science, Palacky University, 78371 Olomouc, Czech Republic
- * Correspondence: franziska.roth-walter@meduniwien.ac.at

Abstract: Bet v 1 is the major allergen in birch pollen to which up to 95% of patients sensitized to birch respond. As a member of the pathogenesis-related PR 10 family, its natural function is implicated in plant defense, with a member of the PR10 family being reported to be upregulated under iron deficiency. As such, we assessed the function of Bet v 1 to sequester iron and its immunomodulatory properties on human immune cells. Binding of Bet v 1 to iron quercetin complexes FeQ2 was determined in docking calculations and by spectroscopy. Serum IgE-binding to Bet v 1 with (holoBet v1) and without ligands (apoBet v 1) were assessed by ELISA, blocking experiments and Western Blot. Crosslinking-capacity of apo/holoBet v 1 were assessed on human mast cells and Arylhydrocarbon receptor (AhR) activation with the human reporter cellline AZ-AHR. Human PBMCs were stimulated and assessed for labile iron and phenotypic changes by flow cytometry. Bet v 1 bound to FeQ2 strongly with calculated Kd values of 1 nM surpassing affinities to quercetin alone nearly by a factor of 1000. Binding to FeQ2 masked IgE epitopes and decreased IgE binding up to 80% and impaired degranulation of sensitized human mast cells. Bet v 1 facilitated the shuttling of quercetin, which activated the anti-inflammatory AhR pathway and increased the labile iron pool of human monocytic cells. The increase of labile iron was associated with an anti-inflammatory phenotype in CD14+ monocytes and downregulation of HLADR. To summarize, we reveal for the first time that FeQ2 binding reduces the allergenicity of Bet v 1 due to ligand masking, but also actively contributes anti-inflammatory stimuli to human monocytes, thereby fostering tolerance. Nourishing immune cells with complex iron may thus represent a promising antigen-independent immunotherapeutic approach to improve efficacy in allergen immunotherapy.

Keywords: holo-Bet v 1; major allergen; immunomodulation; immune resilience; iron; quercetin; birch pollen; pathogenesis-related proteins; innate defense; nutritional immunity



Citation: Regner, A.; Szepannek, N.; Wiederstein, M.; Fakhimahmadi, A.; Paciosis, L.F.; Blokhuis, B.R.; Redegeld, F.A.; Hofstetter, G.; Dvorak, Z.; Jensen-Jarolim, E.; et al. Binding to Iron Quercetin Complexes Increases the Antioxidant Capacity of the Major Birch Pollen Allergen Bet v 1 and Reduces Its Allergenicity. *Antioxidants* **2023**, *12*, 42. <https://doi.org/10.3390/antiox12010042>

Academic Editors: Janka Vašková and Mária Mareková

Received: 12 December 2022
Accepted: 21 December 2022
Published: 26 December 2022



Copyright: © 2022 by the authors. Licensee MDPI, Basel, Switzerland. This article is an open access article distributed under the terms and conditions of the Creative Commons Attribution (CC BY) license (<https://creativecommons.org/licenses/by/4.0/>).

1. Introduction

Not every protein is able to become under natural conditions an allergen. As such, allergens are clustered in protein families with the major allergens from mammalian systems always belonging to the “lipocalin” superfamily [1] and major allergens from plant

origins usually belonging to either the pathogenesis-related proteins PR10 family or to the prolamin superfamily which comprises major allergens from the seed storage protein families being 2S albumins as well as the non-specific lipid transfer proteins nsLTPs [2,3]. Major allergens from plant origin also belong to the Gibberellin-regulated proteins GRPs [4], cupin protein superfamily (legumins-7S and vicilins-11S protein) and Ole e 1 families [5]. In 2012, our group made the serendipity discovery that the major birch pollen allergen Bet v 1 shares a lipocalin-like structure with the endogenous human lipocalin 2 LCN2 [6], which linked one of the largest major plant allergen family with a similar large major mammalian allergen family and with human LCN2. Indeed, LCN2 is decreased in allergic subjects [7] and as innate defense protein is usually present at mucosal surfaces and lymphoid sites. It is involved in numerous iron-dependent and immunoregulatory processes, where it can bind iron, but only when the iron is complexed by catechol-based siderophores, since lipocalins usually have no measurable affinity for iron alone [8]. LCN2's ability to bind to iron makes it an antioxidant as it is able to prevent oxidative stress and prevent ferroptosis [9]. The iron-containing form of LCN2 (holoLCN2) is also present and released by anti-inflammatory macrophages [10] and contributes to tissue healing and recovery upon injury. In contrast, inflammatory macrophages release iron-free apo-LCN2 in response to invading bacteria [10].

In plants, immunity can be triggered via different pathways. One is the recognition via the recognition of pathogen-associated molecular patterns that leads to the induction of antimicrobial proteins, secondary metabolites, reactive oxygen species ROS formation and cell wall reinforcements. The second is the so-called effector-triggered immunity ETI, which can be initiated in plants by the perception of pathogen activity and usually leads to local program cell death named "hypersensitive response" (as a hallmark for systemic acquired resistance [11]). This ETI is triggered by salicylic acid accumulation to limit the pathogen spread [12]. Interestingly, iron depletion in plants is sufficient to prime plant immunity [13] leading to salicylic acid accumulation [13–15] and increasing coumarin and flavonoid synthesis [16–19] as well as the transcription of pathogenesis-related PR genes [15,20–22]. There seems to be a direct link between plant iron homeostasis and PR gene expression as iron treatment downregulates in plants the expression of PR10 proteins [23].

Interestingly, similar to mammalian lipocalins binding to iron via catechol-based siderophores, in 2014 the natural flavonoid ligand of Bet v 1 has been identified as quercetin-3-O-sophoroside [24], which likewise contains a catechol-moiety [25] with a very high affinity to iron [26]. As such, flavonoids seem to be the plant counterpart to bacterial-derived siderophores, with both considered secondary metabolites in the respected plants and bacteria/fungi and having both strong anti-oxidative and anti-inflammatory features, which are linked with their ability to complex iron.

In this respect, we hypothesized that similar to the mammalian lipocalin family, also in plants the natural function of the PR10 protein Bet v 1 is associated with plant iron homeostasis and immunity. We hypothesized that the allergenic or tolerogenic feature of Bet v 1 is linked to its iron-scavenging ability that it can exert cross-species, thereby enabling the modulation of the immune response in human immune cells with the iron-laden versus the iron-free form affecting the allergenicity of Bet v 1.

2. Materials and Methods

2.1. Structural and Docking Analysis

Atom coordinates of Bet v 1 were taken from the high-resolution (1.24 Å) crystal structure of its complex with naringenin (protein data bank (PDB) entry 4A87) [27]. The geometries of quercetin were obtained upon energy minimization with the MM2 force field of initial structures drawn using the ChemBioDraw/ChemBio3D Ultra 12.0 package. Docking input files for protein and ligands were prepared with reduce v3.23 [28], the ADFR software suite (<https://ccsb.scripps.edu/adfr>; accessed on 12 August 2021) and AutoDockTools [29]. Docking calculations were performed with AutoDock Vina [30,31]. The docking solution with the lowest affinity energy E_{aff} was selected. Estimates of dissociation equilibrium

constants K_d were then calculated for the protein-ligand complexes by assuming $E_{\text{aff}} \sim \Delta G$ with $K_d = \exp(-\Delta G/RT)$ at $T = 298.15$. Protein structural visualizations were prepared with UCSF Chimera [32,33].

2.2. Recombinant Bet v 1

Bet v 1 was produced as described [34]. In short, a codon-optimized synthetic gene of Bet v 1.0101 was obtained from Eurofins MWG Operon (Ebersberg, Germany) and cloned into the expression vector pET-28a(+) (Merck Millipore, Darmstadt, Germany). The proteins were expressed in *E. coli* BL21[DE3] in LB medium at 37 °C after induction with 1 mM isopropyl-D-thiogalactopyranoside. Bet v 1 was purified by a combination of hydrophobic interaction and ion exchange chromatography. SDS-PAGE, MALDI-TOF MS (Bruker Ultraflex II, Bruker Daltonics, Billerica, MA, USA), and circular dichroism (CD) spectroscopy was used to verify protein purity and identity, mass, and secondary structure. Measurement of endotoxin content was done by Hyglos EndozymeII Kit (Bernried am Starnberger See, GER) and total protein content by BCA assay according to the manufacturer's instructions (Pierce BCA Protein Assay Kit, Thermo Scientific, Rockford, IL, USA).

2.3. Generation of Apo- and Holo Bet v 1

Bet v 1 (1.1–1.89 mg/mL) was dialyzed three times against 10 μM deferoxamine mesylate salt (Sigma D9533, St. Louis, MO, USA) following dialyzation against deionized water to generate apoBet v 1. HoloBet v 1 was generated by adding pre-formed iron-quercetin complexes (FeQ2). 3 mM FeQ2 complexes were generated by dissolving quercetin (Sigma 1592409) in 1 M NaOH and adding acidic iron (Iron-standard AAS, Sigma 16596) at a ratio 2:1, before adding them to apoBet v 1 to a final concentration of, e.g., 10 μM Bet v 1, 20 μM quercetin and 10 μM iron or dilutions thereof.

2.4. Spectral Analysis

For spectral analysis, a physiological saline solution (0.89% NaCl) was used as a buffer to minimize iron contamination from the air. The pH was kept constant at pH 7 for Figure 1c,d and was >7.3 for Figure 1e–g. Optical density was measured using (1) 200 μM quercetin (=100 μM Q2) with increasing concentrations of ferric iron (40–200 μM), (2) 100 μM FeQ2 with increasing concentrations of Bet v 1 (2–20 μM) or (3) 100 μM FeQ2 with increasing concentrations of gel-filtrated apoBet v 1 or holoBet v 1 (0.5–8 μM). All measurements were repeated at least three times with similar results.

2.5. Anti-Oxidative Assay

Anti-oxidative status was measured as described before [35,36]. Shortly, a 7 mM ABTS radical stock solution was prepared by diluting 19 mg of 2,2'-Azinobis-(3-ethylbenzothiazoline-6-sulfonic acid) (Sigma A1888) (ABTS+) and 20 mg ammonium persulfate (Sigma A3678) in 5 mL distilled water at room temperature. The stock solution was further diluted 1:4 in distilled water to obtain an ABTS working solution. As standard either Trolox (Sigma 238813, Austria, St. Louis, MO, USA), quercetin Q2 or FeQ2 was used. Samples of apoBet v 1 (0.5 mg/mL) and/or preincubated with FeQ2, Q2 or ferroxamine (FO) were subjected to gel filtration (PD MiniTrap G-25 Columns, GE Healthcare 28-9180-07) to remove unbound ligands. 50 μL of diluted samples or diluted standards (Trolox, Q2, FeQ2) were incubated with 50 μL of ABTS working solution for 2 min in a 96 well plate before measurement of absorbance at 740 nm using an Infinite M200Pro microplate reader (Tecan, Grödig, Austria). Data are shown as antioxidative capacity using Trolox-equivalent normalized to apoBet v 1 in Figure 1f,g using FeQ2 and Q2 as standard to calculate the molar ratio of quercetin to Bet v 1.

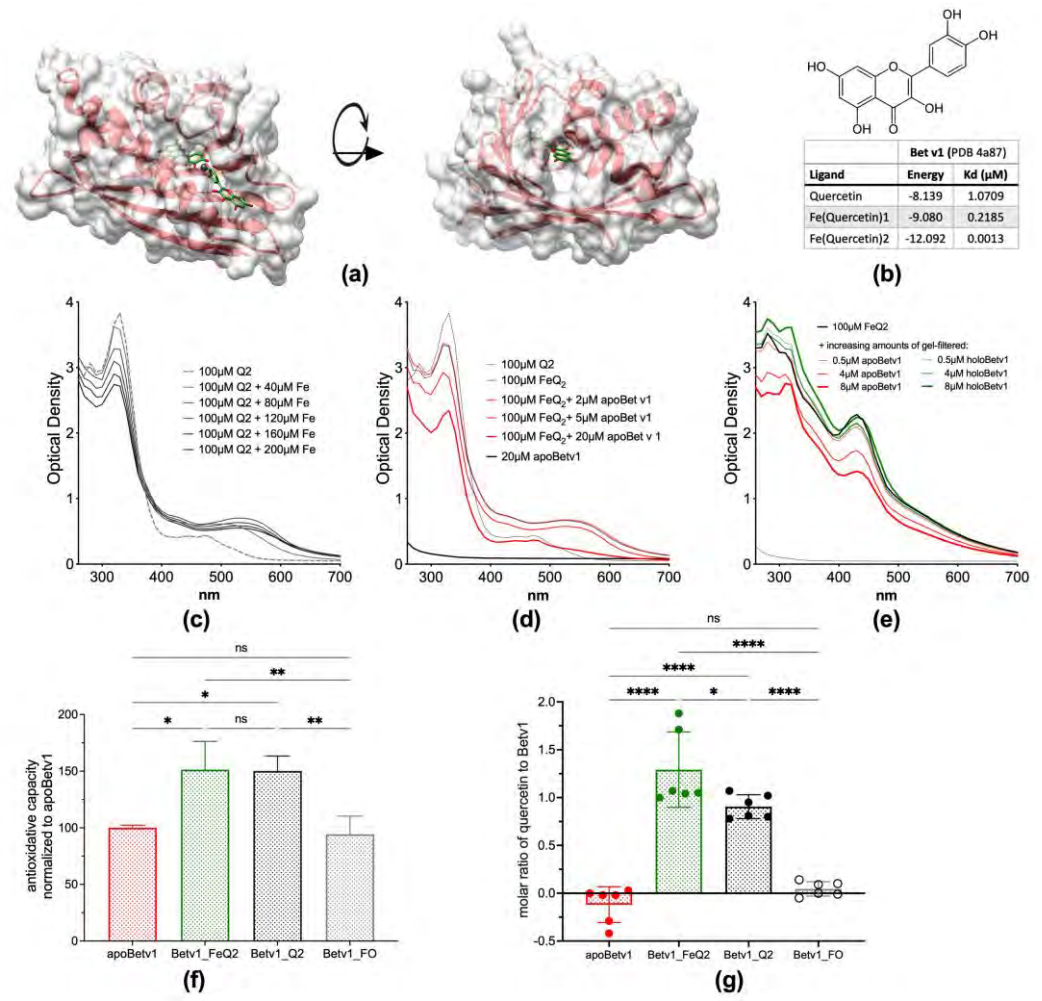


Figure 1. Bet v1-holoBet v1-Quercetin complex (a). Part of the face of the protein surface Bet v1 in conjunction with quercetin (Q) sticks with carbons in green, oxygens in red, and iron shown as a grey sphere (b). Molecular structure of quercetin and calculated affinities of quercetin in conjunction with iron to Bet v1. (c). Optical spectra of 200 μM quercetin (Q) with increasing concentration of ferric iron at pH 7.3. (d). Optical spectra of 20 μM Bet v1, 100 μM FeQ2 alone, or by adding increasing concentrations of Bet v1. (e). FeQ2 spectra with and without the addition of increasing doses of gel-infiltrated purified apoBet v1 or holoBet v1. (f). ApoBet v1 was preincubated with FeQ2, Q or ferroxamine (FO), before removing unbound ligands by gel-filtration and performing a Trolox Equivalent Antioxidant Test using Trolox as reference. (g). ApoBet v1 was preincubated with FeQ2, Q or ferroxamine (FO) before removing unbound ligands by gel-filtration and performing a Trolox Equivalent Antioxidant Test using Trolox as reference. (g) capacity with quercetin amount of bound quercetin to Bet v1. Statistical analyses (f,g) were compared with quercetin and FeQ2 as reference. For statistical analyses, comparisons were completed with a single pooled variance ANOVA followed by Holm-Sidák's multiple comparisons test with a single pooled variance; Mean ± SD; ns not significant; * $p < 0.05$; ** $p < 0.01$; **** $p < 0.0001$.

3.2. IgE Epitopes Masking and Less Mast Cell Degranulation by HoloBet v 1

2.6. Bet v1-Specific Sera

In the next step, we investigated whether the allergenicity of Bet v1 was affected by the addition of quercetin. Serum samples derived from two clinical trials (NCT0381598, NCT03811690) which were approved by the ethics committees and to sampling from the Mast Cell Epitope 1) and 2) patients (3 characteristic) have been described previously in detail [37,38]. Briefly, sera of subjects with pollen rhinitis, but who otherwise were asymptomatic for Bet v1-specificity (Figure 2), as well as sera testing for specific IgE by ALFA[®] (Maccormac Diagnostics, Wien, Austria) and ALFA[®] test specific IgE level against Bet v1 being at least 1 kU_A/L. The concentration of individual sera and in the pools for Bet v1-specific IgE ranged from 10 to 60 kU_A/L (without any ligands) or with the ligands FeQ2 (Betv1_FeQ2), quercetin (Betv1_Q2) or using ferroxamine as a hydroxamate-based siderophore

2.7. *Bet v1-Specific IgE ELISA*

Two $\mu\text{g}/\text{mL}$ of apoBet v 1, holoBet v1-FeQ2, Bet v 1-Q2 or Bet v 1-FO (ferroxamine) diluted in 0.89% NaCl were coated (100 μL per well) overnight at 4 °C, blocked for 2 h at room temperature with 1% BSA in 0.89% NaCl containing 0.05% Tween 20 (200 μL per well), before incubated with 100 μL of diluted serum from birch-pollen allergic and non-allergic subjects (1:10 diluted in 0.89% NaCl/0.05% Tween-20) overnight at 4 °C. Bound IgE was detected with horseradish–peroxidase-conjugated goat anti-human IgE antibody (Invitrogen A18793, Waltham, MA, USA) diluted at 1:4000 in 0.89% NaCl containing 0.05% Tween-20 and using tetramethylbenzidine (eBioscience, San Diego, CA, USA) as a substrate. Color development was stopped with 1.8 M sulfuric acid. The optical density was measured at 405 nm by using an Infinite M200Pro microplate reader (Tecan, Grödig, Austria). Between the steps, rigorous washing was performed with 0.89% NaCl containing 0.05% Tween-20. Data are shown as a percentage normalized to apoBet v 1 IgE binding levels or as OD at 450 nm.

2.8. *Bet v 1-Specific IgE Inhibition ELISA*

Inhibition experiments were carried out similarly as described for the Bet v 1-specific IgE ELISA. Briefly, plates were coated with 2 $\mu\text{g}/\text{mL}$ of apoBet v 1 or holoBet v 1-FeQ2 (100 μL per well) overnight at 4 °C. In the meantime, pooled serum from birch-pollen allergic subjects (diluted 1:10 in 0.89% NaCl) was preincubated with increasing doses of apoBet v 1 (0–1000 ng/mL) or holoBet v 1-FeQ2 (0–1000 ng/mL) also overnight at 4 °C. After washing and blocking, preincubated serum samples were applied (100 μL per well) overnight at 4 °C. Detection was performed by using horseradish–peroxidase-conjugated goat anti-human IgE antibody (Invitrogen A18793) diluted at 1:4000 in 0.89% NaCl containing 0.05% Tween-20, with use of tetramethylbenzidine (eBioscience) as a substrate and 1.8 M sulfuric acid to stop color development. The optical density was measured at 450 nm with the Infinite M200Pro microplate reader (Tecan, Grödig, Austria). Data are shown as OD at 450 nm or as kU/L IgE binding to plate-bound apoBet v 1.

2.9. *SDS-PAGE and Western Blot*

ApoBet v 1 and holoBet v 1-FeQ2 were mixed with 4x non-reducing sample buffer and 12 $\mu\text{g}/\text{slot}$ was applied on two sodium dodecyl sulfate polyacrylamide (SDS–PAGE) 4–20% gradient gels (Biorad 4568095, Tokyo, Japan), run at 90 V for about 1 h and subsequently one gel was stained with Roti-Blue quick solution (Roth 4829.2, Roth, Germany) and the other gel underwent immunoblotting. Briefly, the gel was blotted on a methanol-activated PVDF-membrane (Immobilon IPVH00010, 0.45 μm), blocked with 1% BSA in tris buffered saline containing 0.05% Tween-20 (TBS-T) for 18 h, before incubating with 1:10 diluted serum pool of allergic donors ($n = 17$) for 18 h at 4 °C. Bound IgE was detected with horseradish peroxidase labeled anti-human IgE antibody (Invitrogen A18793) and using ECL substrate (clarity TM Western ECL Substrate, BioRad 170-5061) for detection. Between each step, rigorous washing was performed with TBS-T. Luminescence was imaged with the ChemiDoc™ Touch Imaging System (BioRad).

2.10. *Human Mast Cell Degranulation Assay*

Human peripheral blood mononuclear cell-derived mast cells were generated as previously described by Folkerts et al. [39]. Briefly, peripheral blood mononuclear cells were obtained from buffy coats of healthy blood donors and CD34+ precursor cells were isolated using the EasySep Human CD34 Positive Selection Kit (STEMCELL Technologies). CD34+ cells were maintained for 4 weeks under serum-free conditions using StemSpan medium (STEMCELL Technologies) supplemented with recombinant human IL-6 (50 ng/mL; Peprotech), human IL-3 (10 ng/mL; Peprotech) and human Stem Cell Factor (100 ng/mL Peprotech, Rocky Hill, NJ, USA). After 4 weeks, the cells were cultured in Iscove's modified Dulbecco's medium/0.5% bovine serum albumin with human IL-6 (50 ng/mL, Peprotech, Rocky Hill, NJ, USA) and 3% supernatant of Chinese hamster ovary transfectants secret-

ing murine stem cell factor (a gift from Dr. P. Dubreuil, Marseille, France). The mature MCs were identified by flow cytometry based on positive staining for CD117 (eBioscience) and FcεRIa (eBioscience) using BD FACS Canto II (approximately 90%). Degranulation assay was performed by incubation of human mast cells with serum pools of birch pollen allergic or non-allergic subjects followed by incubation with 5 nM of apoBet v 1, holoBet v1, Q2, FeQ2 or buffer, respectively. Degranulation was assessed by measurement of the activity of released β-hexaminidase in the supernatant and unreleased enzyme in the respective cell lysate. The presented results were calculated as percentage released versus total β-hexaminidase activity, with a release from unstimulated controls being 0.003%, from positive controls with anti-human IgE being 33.4% and with ionomycin being 84.6%.

2.11. AZ-AhR Reporter Assay

AZ-AhR assay was done as previously described [40]. Briefly, AZ-AhR cells were plated on 96-well plates at a density of 2×10^4 cells/well for 18 h. Subsequently, cells were stimulated for 18 h in triplicates with 45 μM of iron-queracetin complexes alone or in addition with 2 μM or 10 μM Bet v 1. The positive control cells were treated with 20 nM indirubin. Cells were washed once with 0.89% NaCl, before the lysis buffer of the luciferase assay kit (Promega E4530, Tokyo, Japan) was added. After a single freeze-thaw cycle, 20 μL/well of lysates were transferred into a black 96-well flat-bottom plate (Thermo Scientific) and bioluminescent reaction were started with addition of 100 μL/well of luciferase assay reagent (Promega). Chemiluminescence was measured (10 s/well) using a spectrophotometer (Tecan InfiniteM200 PRO). Data from six independent experiments are shown as normalized to medium levels.

2.12. Flow Cytometric Analysis of Human PBMCs

PBMCs were isolated by Ficoll-Paque (GE Healthcare) and washed with 0.9% NaCl before incubation with 5 μM iron-queracetin (FeQ2) alone and/or in combination with 5 μM apoBet v1 in media containing neither phenol red nor FCS for 18 h as previously described [41]. Subsequently, cells were stained with combinations of calcein-AM (ThermoFisher, Waltham, MA, USA), CD3-APC-Cy7 (eBioscience, clone SK7), CD14-APC-Cy7 (Biolegend, clone M5EZ), HLADR-PE (Biolegend, San Diego, Calif, clone L243PC), and CD86-PE-CY7 (Biolegend, clone IT2.2) for flow cytometric analysis. Calcein-AM violet was used as a living marker and to determine the labile iron load in living cells. Doublets were excluded before gating on CD3+ cells in the lymphocyte population or on CD14+ cells in the monocytic population. In monocytic cells this was followed by consecutive gating for HLADR+, CD86+ and calcein+ and geometric mean fluorescence intensity (MFI) was calculated for each fluorochrome. Acquisition and analyses were performed on a FACS Canto II machine (BD Bioscience, San Jose, CA, USA) using the FACSDiva Software 6.0 (BD Biosciences).

2.13. Statistical Analyses

Anti-oxidative assay and mast cell degranulation were compared with one-way ANOVA following Holm-Sidák's multiple comparisons test, with a single pooled variance. Data from IgE ELISA were compared with RM one-way ANOVA with Geisser Greenhouse correction and Holm-Sidák's multiple comparisons test and inhibition ELISA with two-way ANOVA using Holm-Sidák's multiple comparisons test, with a single pooled variance. AhR activation and flow cytometry of PBMCs was analyzed by mixed-effect analysis or with RM one-way ANOVA including Geisser-Greenhouse correction followed by Tukey's multiple comparisons test. All tests were considered significant when $p < 0.05$. Statistical analysis was performed with Graphpad prism 9.4.1 (San Diego, CA 92108, USA).

3. Results

3.1. Bet v 1 Binds Strongly to Iron-Quercetin Complexes In Silico and In Vitro

The natural ligand of Bet v 1 has been isolated with a quercetin-core structure [24], with quercetin known to act as a very strong iron chelator [42]. The binding of this ligand transforms Bet v 1 from apo- (empty) to holo-Bet v 1. Quercetin alone has anti-inflammatory properties itself, and from previous studies [6,41,43], we hypothesized that the binding of this immunomodulatory molecule in conjunction with iron would modify the allergenicity of Bet v 1. In the first step, we proved by different means that Bet v 1 binds to iron-quercetin complexes (FeQ2). In silico analysis revealed that Bet v 1 binds by a factor of 10^3 stronger to FeQ2 compared to quercetin alone by (Figure 1a,b). The calculated FeQ2 binding affinity energy was -12.092 kcal/mol, corresponding to a dissociation constant K_d of 0.0013 $\mu\text{mol/L}$, whereas binding to quercetin alone has an affinity energy of -8.139 kcal/mol, corresponding to a K_d of 1.0709 $\mu\text{mol/L}$.

Additionally, by spectroscopical means iron-quercetin complex formation was visible (Figure 1c). Binding to FeQ2 could be proven, because a second absorption maximum diminished concentration-dependently upon addition of apoBet v 1 (empty protein, no ligand) (Figure 1d), but not when holoBet v 1 (protein-ligand complex) was added (Figure 1e). After removing potential unbound ligands by gel filtration, we show that the antioxidative capacity of Bet v 1 increased due to binding to the ligands FeQ2 and quercetin, which allowed also to compute the number of bound ligands per Bet v 1 molecule, being 1.29 ± 0.39 for FeQ2 complexes and 0.90 ± 0.12 for quercetin (Figure 1f,g). To sum up, we provide evidence, that Bet v1 strongly binds to iron-quercetin complexes at physiological relevant pH.

3.2. IgE Epitopes Masking and Less Mast Cell Degranulation by Holobet v 1

In the next step, we investigated whether the allergenicity of Bet v1 was affected by binding to iron—quercetin complexes. Bet v1 has two described IgE epitopes to which birch pollen allergic IgE antibodies bind to spanning, from aa29 to aa58 (epitope 1) and from aa73 to aa103 (epitope 2) [44]. In silico analysis revealed that both IgE epitopes were affected by FeQ2: epitope 1 at Phe 30 and Phe 58 and epitope 2 at Tyr 81, Tyr83 and Ile 102. (Figure 2a) similar as described for FeQ2 binding masking major lipocalin allergens [40,41]. Next, we verified the biological relevance of the in silico findings, by testing whether individual IgE of birch pollen allergic patients ($n = 12$) bound similarly to plate-bound apoBet v1 (without any ligands) or with the ligands FeQ2 (Betv1_FeQ2), quercetin alone (Betv1_Q2) or using ferroxamin complexes as a hydroxamate-based siderophore-iron complex to which Bet v1 should not bind to (Betv1_FO) as control. Indeed, a significant reduction in IgE-binding was very apparent against holoBet v 1 with FeQ2 and to a lesser degree also to quercetin alone (Figure 2b). Additionally, in blocking experiments with pooled sera preincubated with various doses of apoBet v 1, the binding to plate-bound holoBet v 1 was significantly reduced compared to apoBet v 1 (Figure 2c). In blocking experiments when individual sera ($n = 6$) were preincubated with various concentrations of apo- or holo-Bet v 1 a significantly greater blocking (Supplementary Figure S1). Thus reduced IgE-binding was achieved with the apo-form—as depicted in the summary graph and confidence interval plot in Figure 2d—and highlights that IgE epitopes were masked and not accessible with the holo-form (Figure 2d). A similar pattern was evident in Western Blot, with a reduced IgE-binding (using pooled sera) seen when Bet v 1 was in conjunction with FeQ2 (Figure 2e). Moreover, when human-generated mast cells were sensitized with sera of birch pollen allergic sera, crosslinking with holoBet v1 compared to apoBet v 1 was less efficient and resulted in significantly less degranulation. No degranulation was achieved when mast cells were sensitized with non-allergic sera, (Figure 2f,g).

IgE-binding was achieved when mast cells were sensitized with non-allergic sera, (Figure 2f,g).
 and confidence interval plot in Figure 2d—and highlights that IgE epitopes were masked and not accessible with the holo-form (Figure 2d). A similar pattern was evident in Western Blot, with a reduced IgE-binding (using pooled sera) seen when Bet v 1 was in conjunction with FeQ2 (Figure 2e). Moreover, when human-generated mast cells were sensitized with sera of birch pollen allergic sera, crosslinking with holoBet v1 compared to apoBet v1 was less efficient and resulted in significantly less degranulation. No degranulation was achieved when mast cells were sensitized with non-allergic sera, (Figure 2f,g).

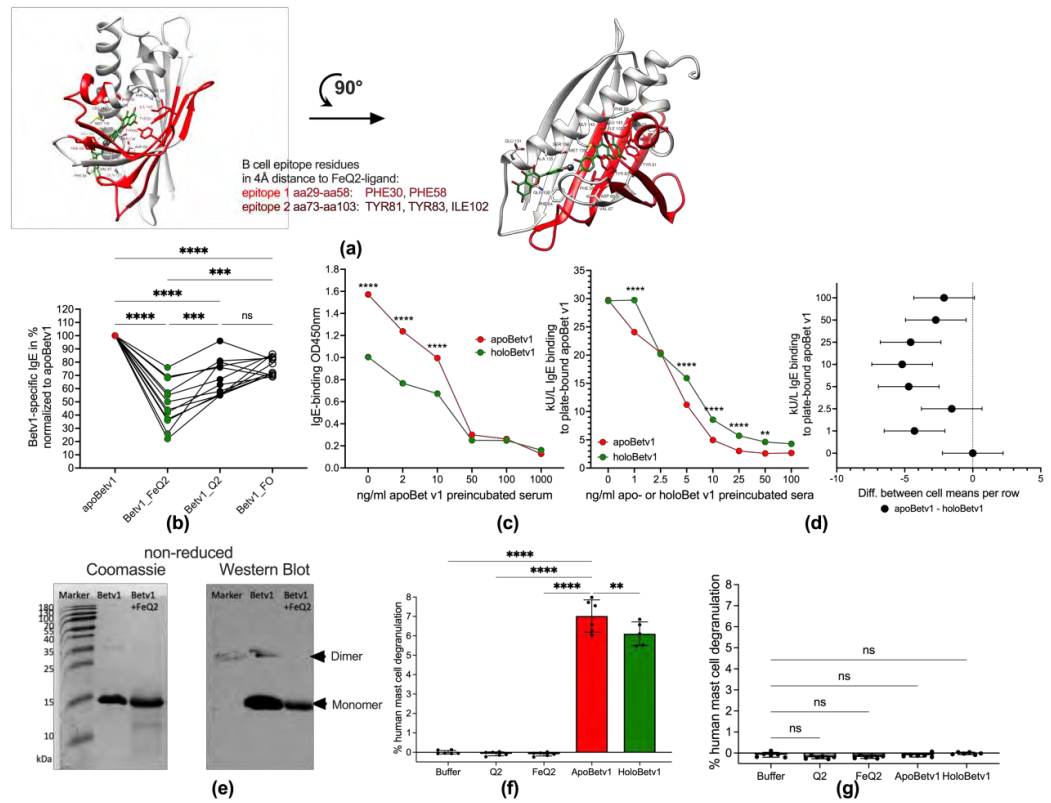


Figure 2. Binding of iron-Fe(II)-quercetin complex by Bet v 1 and its effect on IgE binding and mast cell degranulation. (a): Structure of Bet v 1-Fe(II)-quercetin complex shown as cartoon from two different views. Iron complexed by two quercetins (FeQ2) is depicted as sticks with carbons in green and oxygens in red. Iron atom (Fe) is represented as a grey sphere. Major B cell epitope 1 (29–58) and epitope 2 (73–103) are marked in light and dark red, respectively. Residues within a 4Å distance from any atom of FeQ2 are shown as sticks with carbons in red. (b): Serum IgE binding of birch pollen allergic (n = 12) to Bet v 1 without cargo (apoBet v 1) or in combination with iron-Fe(II)-quercetin (FeQ2), quercetin (Q2), or ferroxamine (FeO). (c): Blocking experiments of birch pollen allergic (n = 12) to Bet v 1 without cargo (apoBet v 1) or in combination with iron-Fe(II)-quercetin (FeQ2), quercetin (Q2), or ferroxamine (FeO). (d): Summary and confidence interval plot of blocking experiments incubating 6 individual sera of birch pollen allergic subjects with increasing doses of apo- (red line) or holoBet v 1 (green line). (e): Protein bands stained by Coomassie and serum IgE binding against Bet v 1 alone or in combination with FeQ2 of gels run under non-reducing conditions. Degranulation of human mast cells sensitized with pooled (f) birch pollen allergic (g): non-allergic sera. For statistical analyses (b) was compared with RM one-way ANOVA with Geissner Greenhouse correction and Holm-Sidák’s multiple comparisons test (c,d) with two-way ANOVA using Holm-Sidák’s multiple comparisons test, with a single pooled variance, (f) with mixed-effect analyses using the Geissner Greenhouse correction and Holm-Sidák’s multiple comparisons test, (g) with one-way ANOVA following Holm-Sidák’s multiple comparisons tes. Mean ± SD; ns not significant, ** p < 0.01, *** p < 0.001, **** p < 0.0001.

3.3. Bet v 1 Facilitates Quercetin-Dependent AhR Activation—And Iron Transport into Human Cells

Next, we aimed to prove that the ligands were responsible for the reduced allergenic features of Bet v 1 and that in fact the uptake of these ligands into human immune cells was facilitated by Bet v 1. To prove that Bet v 1 facilitated quercetin-transport into human cells, the human AZ-AhR cell line stably transfected with several aryl hydrocarbon-receptor AhR binding sites upstream of the luciferase reporter gene [45] were stimulated with apo-/holo-Bet v 1, as quercetin is a known activator of AhR. Indeed, the activity of AhR concentration-dependently increased by the addition of Bet v 1 from 3.0 ± 1.4 with FeQ2

alone to 5.6 ± 2.6 with $2 \mu\text{M}$ and to 10.84 ± 7.1 with $10 \mu\text{M}$ Bet v 1 (Figure 3a). To proof that not only quercetin, but also iron was transported into human immune cells, PBMCs from allergic donors ($n = 34$) were stimulated with apo/holoBet v 1. Indeed, though Bet v 1 led to an increase in cell survival (Supplementary Figure S2) in the lymphocytic compartment and led to the relative expression of CD3+, this was irrespective of the ligand and also the labile iron pool, measured by the quenching of the Calcein-signal—was not affected (Figure 3b,c). In contrast, relative CD14 expression decreased upon Bet v 1 exposure but further significantly decreased in PBMCs incubated with holoBet v 1 compared to cells stimulated with apoBet v 1 only. Moreover, holoBet v 1 incubation led to a significant increase of the labile iron in monocytes with PBMCs being unaffected by apoBet v 1 and also by incubation of FeQ2 alone (Figure 3d,e). Importantly, the relative numbers of living cells did not differ between apo- and holoBet v 1 incubated cells (Supplementary Figure S2). To sum up, here we show that Bet v 1 was able to shuttle quercetin as well as iron into human cells, thereby on the one hand activating the anti-inflammatory AhR pathway and on the other hand increasing the labile iron of CD14+ cells, but not of CD3+ cells.

Antioxidants 2022, 11, x FOR PEER REVIEW

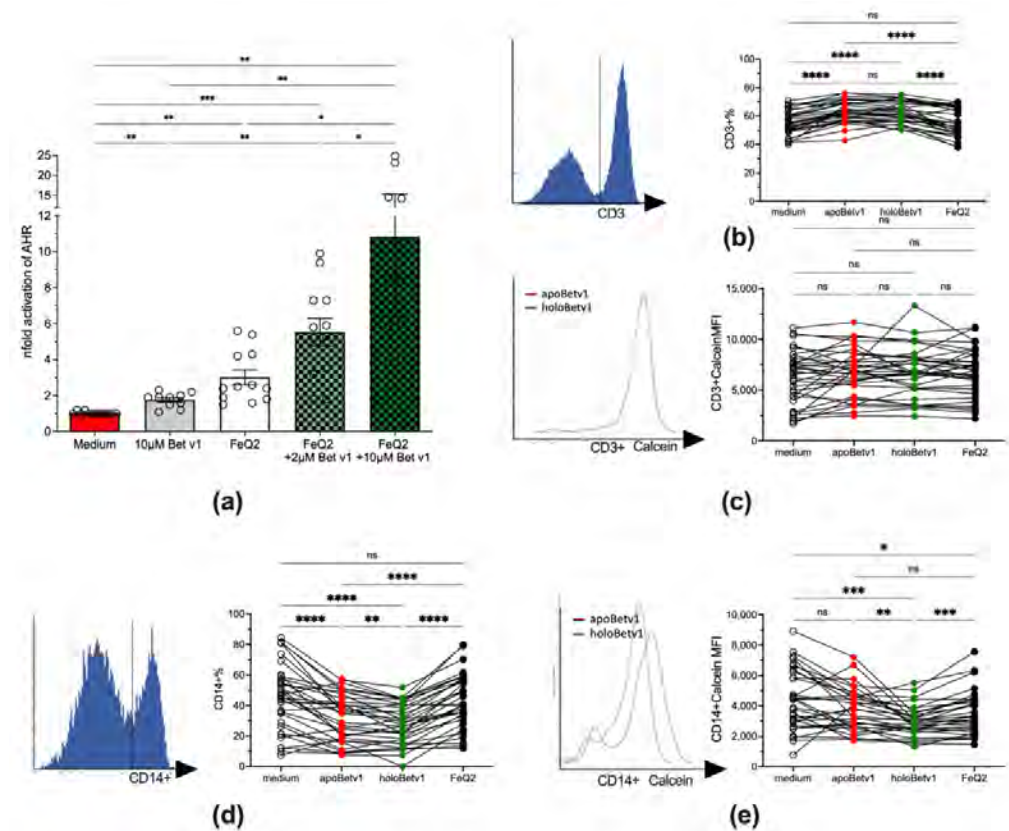


Figure 3. Shuttling of FeQ2 by Bet v 1 activates the anti-inflammatory aryl hydrocarbon receptor and increases labile iron in monocytes. (a) AhR activation by quercetin iron complex is increased upon addition of Bet v 1. (b) Gated CD3+ cells and summary of relative CD3+ expression and (c) mean fluorescence intensity (MFI) of the calcein signals thereof. (d) Gating and summary of relative numbers of CD14+ expression as well as (e) MFI of the calcein signals of stimulated CD14+ cells. Data were analyzed in (a,d,e) by mixed-effect analysis and (b,c) with RM one-way ANOVA. All data were Geisser-Greenhouse corrected and followed by Tukey’s multiple comparisons test. * $p < 0.05$; ** $p < 0.01$; *** $p < 0.001$; **** $p < 0.0001$; ns = not significant.

We further assessed the impact of iron-shuttling by Bet v 1 on antigen presentation by assessing labile iron and the expression of HLA-DR as well as the costimulatory molecule CD86 in CD14+ cells. Along with the increase of labile iron also the maturation state of the CD14+ cells changed with a significantly less mature state of CD14+HLA-DR+CD86+ cells observed in holoBet v 1-stimulated PBMCs (Figure 4a,b). Particularly CD14+ with HLA-DR^{low} are attributed to an immunosuppressive phenotype [46]. An increase of the

3.4. Bet v 1 Acts Immunomodulatory by Importing Iron and Suppressing Antigen Presentation

We further assessed the impact of iron-shuttling by Bet v 1 on antigen presentation by assessing labile iron and the expression of HLADR as well as the costimulatory molecule CD86+ in CD14+ cells. Along with the increase of labile iron also the maturation state of the CD14+ cells changed with a significantly less mature state of CD14+HLADR+CD86+ cells observed in holoBet v 1-stimulated PBMCs (Figure 4a,b). Partic-
 antigen presenting skills were associated in regression analyses with a decrease of labile iron (Figure 4e). An increase of the labile iron was especially associated with a decrease in HLADR expression, which was not seen with GD86 (Figure 4a,d). As such, relative numbers of mature monocytes with antigen presenting skills were associated in regression analyses with a decrease of labile iron (Figure 4e).

Antioxidants 2022, 11, x FOR PEER REVIEW

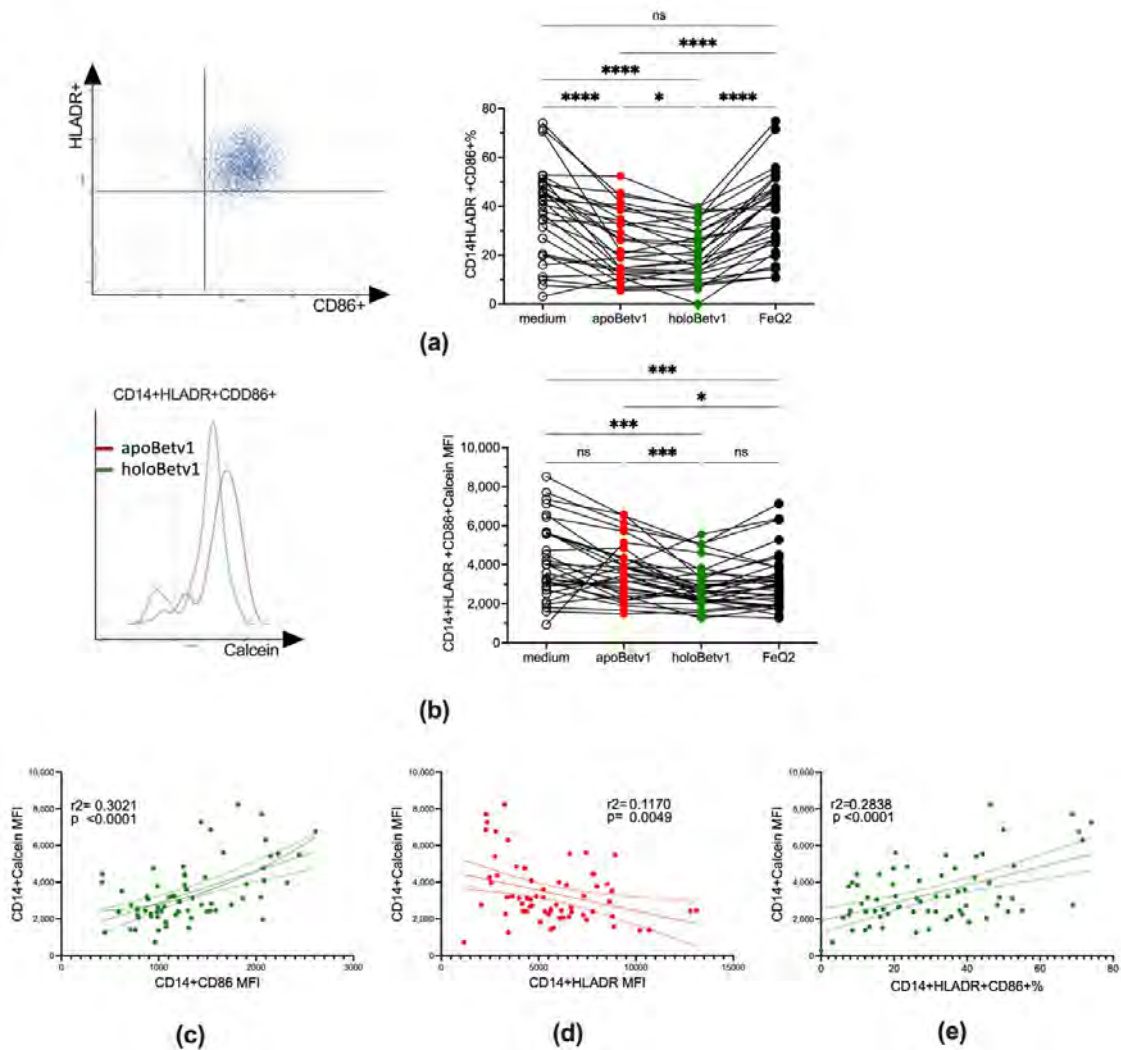


Figure 4. HoloBet v 1 decreased antigen presentation is associated with an increase of labile iron in monocytes. PBMCs were primed with LPS (100 ng/ml) and stimulated with holoBet v 1 (100 ng/ml) in the presence of FeQ2 (100 ng/ml) or apoBet v 1 (100 ng/ml) alone or in combination thereof (holoBet v 1). (a) gating strategy and relative numbers of CD14+HLADR+CD86+ (in the monocytic gate) and (b) the respective MFI of the calcein signal. Linear regression analysis of the Calcein signal of CD14+ cells (c) versus CD86 expression and (d) HLADR expression as well as (e) calcein signal of CD14+ with the relative numbers of CD14+HLADR+CD86+ cells. Data were analysed in (a,b) by mixed-effect analysis. All data were Geisser-Greenhouse corrected and followed by Tukey’s multiple comparisons test. (c–e). Simple linear regression models of data with 95% confidence bands are depicted. * $p < 0.05$; *** $p < 0.001$; **** $p < 0.0001$; ns = not significant.

Hence, we show that shuttling of labile iron by Bet v 1 strongly affected the maturation state of monocytic cells keeping them immature and repressing antigen presentation.

4. Discussion

The present study supports our notion that the natural function of Bet v 1 is strongly linked with its ability to bind to complexes of iron, a redox-active element essential for most life [43]. The strong inherent affinity of particularly ferric iron to flavonoids/polyphenols is highlighted by the fact that flavonoid-iron complexes can self-assemble into huge polyphenol-metal networks [47,48], which is used in the industry to coat microorganisms, but also by the fact that solubilized iron-flavonoid complexes serve as an iron source for commensal and opportunistic microbial pathogens [42]. Importantly, in plants intracellular iron depletion is sufficient to lead to the expression of pathogenesis-related proteins [15,20–22], further emphasizing that the natural function of Bet v 1 is linked with plant defense and nutritional immunity (particularly of iron), similarly as the mammalian counterpart LCN2. Indeed, using the cow milk lipocalin protein beta-lactoglobulin, we could show in previous *in vivo* [40,49] and in clinical studies [38,50,51] that nutritional support to immune cells was essential to induce immune resilience, amelioration of symptoms and tolerance in allergic rhinitis patients.

Here, we show similarly, that the binding affinity to quercetin-iron by Bet v 1 is exceptionally high with calculated affinity being in the lower nM-range, which is about 1000× stronger than to quercetin alone. Moreover, we show that binding to iron-quercetin complexes was superior to quercetin alone in hampering epitope-recognition by specific IgE antibodies from birch pollen-allergic individuals. Importantly, this had also implications for the effector phase as crosslinking by holoBet v 1 was not as effective as with apoBet v 1 without any ligands, in which epitope masking did not hinder crosslinking. It also indicates that during allergic sensitization Bet v 1 was presented to the human immune system without any ligand, as otherwise the generation of IgE against these epitopes would have been impeded.

In our study, the impact of the iron-quercetin ligand on rendering Bet v 1 less allergenic was not restricted on IgE recognition. Indeed, here we give evidence that the carrier function of Bet v 1 is crucial to provide an anti-inflammatory and anti-oxidative stimulus to human immune cells. Both the transport of quercetin as well as iron was facilitated by Bet v 1 with quercetin able to activate the arylhydrocarbon receptor, but also to increase the labile iron pool in human monocytic cells, in which a large labile iron pool is a major characteristic of anti-inflammatory macrophages [43].

Activation of the cytoplasmic promiscuous AhR, which interacts with a plethora of exogenous ligands including quercetin [52], is described to mediate anti-inflammatory stimuli [53] that promote regulatory T [54,55], but not Th2 [56] cell differentiation and, keep antigen-presenting cells such as dendritic cells or macrophages in an immature state [57].

Iron seems to have a similar impact- when not present in a free form to generate reactive oxygen species- with an increase of the labile iron content in macrophages promoting an anti-inflammatory phenotype and iron depletion promoting an inflammatory phenotype [58,59]. Indeed, iron deficiency is associated *in vitro* [60–62] and in human clinical studies with Th2 inflammation [63–69]. Iron is also central to the human immune defense, which is highlighted by the fact that the macrophages are the central hub for iron handling, recycling and distribution [70]. Importantly, iron distribution and recycling stops when the macrophage changes due to immune activation to an inflammatory phenotype. As such, both too much and too low intracellular iron levels have been reported to cause oxidative damage in mitochondria and trigger the expression of inflammatory-related genes [71]. This also explains that in humans every chronic immune activation will lead over time to anemia of chronic inflammation [43]. Despite the phylogenetic distance between plants and human, the innate immune mechanisms are evoked by the same triggers, with not only humans being affected by a hypersensitive response towards allergens, but also plant mounting a hypersensitive response that leads to the expression of pathogenesis-

related proteins in response to iron sequestration. Although this immune priming is a very desirable response to infections, it also turns otherwise harmless proteins into allergens.

Our current understanding indicates that the major birch pollen allergen Bet v 1—as a prime example of pathogenesis-related proteins [72]—has the ability to sequester iron, similarly to the mammalian lipocalin family is able to bind iron, and that exactly this feature makes them potent allergens. When they do not carry ligands, they are able to deprive their surrounding of iron complexes, thereby actively leading to immune activation and inflammation [70]. In contrast, when they do carry iron, they indeed are able to augment the labile iron pool in macrophages and thereby promote an immature, tolerogenic and anti-inflammatory phenotype in macrophages [58].

5. Conclusions

To summarize, we reveal for the first time that FeQ2 binding reduces the allergenicity of Bet v 1. We provide evidence that both iron and quercetin are shuttled by Bet v 1 into human immune cells thereby hindering the activation of monocytes by increasing the labile iron levels. The present data are in line with our findings that Bet v 1 can transport micronutrients and thereby promotes tolerance. As such, the principle of nourishing immune cells with micronutrients in an antigen-non-specific manner may be one immunotherapeutic approach to improve efficacy.

6. Patents

FRW, LFP and EJJ declare inventorship of EP2894478 (Roth-Walter F et al., Method and means for diagnosing and treating allergy.) (applicant Biomedical International R+D GmbH, Vienna, Austria). EJJ declares shareholdership in Biomedical Int. R+D GmbH, Vienna, Austria.

Supplementary Materials: The following supporting information can be downloaded at: <https://www.mdpi.com/article/10.3390/antiox12010042/s1>, Figure S1: Serum of 6 birch pollen allergic subjects were incubated with increasing concentration of apo- or holoBet v 1, before assessing the ability of the serum to bind to plate-bound apoBet v1.; Figure S2: No significant differences in the relative numbers of living cells in the gated cell population upon apo- or holoBet v1 stimulation. Peripheral blood mononuclear cells were incubated overnight in iron-free media alone or with quercetin, iron-quercetin in the presence or absence of apoBet v1.

Author Contributions: A.R. performed major parts of experiments, analyzed data and contributed to writing. N.S., A.F., G.H. and K.H. performed experiments, analyzed data and contributed with support and to the writing, B.R.B. and F.A.R. performed mast cell experiments, analyzed data and contributed to writing; M.W. and L.F.P. performed in silico analyzes and contributed to writing, Z.D. provided reporter cell lines and protocols, provided support and contributed to writing, E.J.-J. provided support and contributed to writing, F.R.-W. conceptualized the study, contributed in experiments, designed and directed the study, analyzed part of the data and wrote the manuscript. All authors have read and agreed to the published version of the manuscript.

Funding: The study was partly supported by Biomedical Int. R+D GmbH, Vienna, Austria and by Bencard Allergy GmbH, Munich, Germany. A.F. and K.H. were supported by the Danube Allergy Research Cluster-DARC #08 of the Karl-Landsteiner University, Krems, Austria, to E.J.-J.

Institutional Review Board Statement: The study was approved by the ethics committee (#1972/2017 and #1370/2018) of the Medical University of Vienna and conducted in accordance with the Helsinki Declaration of 1975.

Informed Consent Statement: Informed consent was obtained from all subjects involved in the study.

Data Availability Statement: The data presented in this study are all contained within the article.

Conflicts of Interest: F.R.-W., L.F.P. and E.J.-J. declare inventorship of EP2894478 (Roth-Walter F et al., Method and means for diagnosing and treating allergy.) (applicant Biomedical International R+D GmbH, Vienna, Austria). E.J.-J. declares shareholdership in Biomedical Int. R+D GmbH, Vienna, Austria. F.R.-W. received research funding from Biomedical International R+D GmbH, Vienna, Austria, Bencard Allergie GmbH, Munich, Germany and Vienna, Austria, and Allergy Therapeutics, Worthing, UK. Moreover, she received lecture honoraria by Bencard Allergie GmbH, Munich, Germany and Vienna, Austria, and Allergy Therapeutics, Worthing, UK. The other authors declare no relevant conflict of interest in relation to this publication.

References

- Jensen-Jarolim, E.; Pacios, L.; Bianchini, R.; Hofstetter, G.; Roth-Walter, F. Structural similarities of human and mammalian lipocalins, and their function in innate immunity and allergy. *Allergy* **2016**, *71*, 286–294. [[CrossRef](#)] [[PubMed](#)]
- Missaoui, K.; Gonzalez-Klein, Z.; Pazos-Castro, D.; Hernandez-Ramirez, G.; Garrido-Arandia, M.; Brini, F.; Diaz-Perales, A.; Tome-Amat, J. Plant non-specific lipid transfer proteins: An overview. *Plant Physiol. Biochem.* **2022**, *171*, 115–127. [[CrossRef](#)]
- Shewry, P.R.; Beaudoin, F.; Jenkins, J.; Griffiths-Jones, S.; Mills, E.N.C. Plant protein families and their relationships to food allergy. *Biochem. Soc. Trans.* **2002**, *30*, 906–910. [[CrossRef](#)] [[PubMed](#)]
- Iizuka, T.; Barre, A.; Rougé, P.; Charpin, D.; Scala, E.; Baudin, B.; Aizawa, T.; Sénéchal, H.; Poncet, P. Gibberellin-regulated proteins: Emergent allergens. *Front. Allergy* **2022**, *3*, 877553. [[CrossRef](#)]
- Radauer, C.; Breiteneder, H. Evolutionary biology of plant food allergens. *J. Allergy Clin. Immunol.* **2007**, *120*, 518–525. [[CrossRef](#)] [[PubMed](#)]
- Roth-Walter, F.; Gomez-Casado, C.; Pacios, L.F.; Mothes-Luksch, N.; Roth, G.A.; Singer, J.; Diaz-Perales, A.; Jensen-Jarolim, E. Bet v 1 from birch pollen is a lipocalin-like protein acting as allergen only when devoid of iron by promoting Th2 lymphocytes. *J. Biol. Chem.* **2014**, *289*, 17416–17421. [[CrossRef](#)] [[PubMed](#)]
- Roth-Walter, F.; Schmutz, R.; Mothes-Luksch, N.; Lemell, P.; Zieglmayer, P.; Zieglmayer, R.; Jensen-Jarolim, E. Clinical efficacy of sublingual immunotherapy is associated with restoration of steady-state serum lipocalin 2 after SLIT: A pilot study. *World Allergy Organ. J.* **2018**, *11*, 21. [[CrossRef](#)]
- Devireddy, L.R.; Gazin, C.; Zhu, X.; Green, M.R. A Cell-Surface Receptor for Lipocalin 24p3 Selectively Mediates Apoptosis and Iron Uptake. *Cell* **2005**, *123*, 1293–1305. [[CrossRef](#)]
- Meier, J.; Schnetz, M.; Beck, S.; Schmid, T.; Dominguez, M.; Kalinovic, S.; Daiber, A.; Brüne, B.; Jung, M. Iron-Bound Lipocalin-2 Protects Renal Cell Carcinoma from Ferroptosis. *Metabolites* **2021**, *11*, 329. [[CrossRef](#)]
- Mertens, C.; Kuchler, L.; Sola, A.; Guiteras, R.; Grein, S.; Brüne, B.; Von Knethen, A.; Jung, M. Macrophage-Derived Iron-Bound Lipocalin-2 Correlates with Renal Recovery Markers Following Sepsis-Induced Kidney Damage. *Int. J. Mol. Sci.* **2020**, *21*, 7527. [[CrossRef](#)]
- Ali, S.; Ganai, B.A.; Kamili, A.N.; Bhat, A.A.; Mir, Z.A.; Bhat, J.A.; Tyagi, A.; Islam, S.T.; Mushtaq, M.; Yadav, P.; et al. Pathogenesis-related proteins and peptides as promising tools for engineering plants with multiple stress tolerance. *Microbiol. Res.* **2018**, *212–213*, 29–37. [[CrossRef](#)] [[PubMed](#)]
- Herlihy, J.H.; Long, T.A.; McDowell, J.M. Iron homeostasis and plant immune responses: Recent insights and translational implications. *J. Biol. Chem.* **2020**, *295*, 13444–13457. [[CrossRef](#)] [[PubMed](#)]
- Trapet, P.L.; Verbon, E.H.; Bosma, R.R.; Voordendag, K.; Van Pelt, J.A.; Pieterse, C.M.J. Mechanisms underlying iron deficiency-induced resistance against pathogens with different lifestyles. *J. Exp. Bot.* **2021**, *72*, 2231–2241. [[CrossRef](#)] [[PubMed](#)]
- Shen, C.; Yang, Y.; Liu, K.; Zhang, L.; Guo, H.; Sun, T.; Wang, H. Involvement of endogenous salicylic acid in iron-deficiency responses in Arabidopsis. *J. Exp. Bot.* **2016**, *67*, 4179–4193. [[CrossRef](#)] [[PubMed](#)]
- Aznar, A.; Chen, N.; Rigault, M.; Riache, N.; Joseph, D.; Desmaële, D.; Mouille, G.; Boutet, S.; Soubigou-Taconnat, L.; Renou, J.-P.; et al. Scavenging Iron: A Novel Mechanism of Plant Immunity Activation by Microbial Siderophores. *Plant Physiol.* **2014**, *164*, 2167–2183. [[CrossRef](#)]
- Waters, B.M.; Amundsen, K.; Graef, G. Gene Expression Profiling of Iron Deficiency Chlorosis Sensitive and Tolerant Soybean Indicates Key Roles for Phenylpropanoids under Alkalinity Stress. *Front. Plant Sci.* **2018**, *9*, 10. [[CrossRef](#)]
- Fraser, C.M.; Chapple, C. The Phenylpropanoid Pathway in Arabidopsis. *Arab. Book* **2011**, *9*, e0152. [[CrossRef](#)]
- Wasli, H.; Jelali, N.; Saada, M.; Ksouri, R.; Cardoso, S. Insights on the Adaptation of *Foeniculum vulgare* Mill to Iron Deficiency. *Appl. Sci.* **2021**, *11*, 7072. [[CrossRef](#)]
- Verbon, E.H.; Trapet, P.L.; Stringlis, I.A.; Kruijs, S.; Bakker, P.A.; Pieterse, C.M. Iron and Immunity. *Annu. Rev. Phytopathol.* **2017**, *55*, 355–375. [[CrossRef](#)]
- Liu, G.; Greenshields, D.L.; Sammynaiken, R.; Hirji, R.N.; Selvaraj, G.; Wei, Y. Targeted alterations in iron homeostasis underlie plant defense responses. *J. Cell Sci.* **2007**, *120*, 596–605. [[CrossRef](#)]
- Dellagi, A.; Segond, D.; Rigault, M.; Fagard, M.; Simon, C.; Saindrenan, P.; Expert, D. Microbial Siderophores Exert a Subtle Role in Arabidopsis during Infection by Manipulating the Immune Response and the Iron Status. *Plant Physiol.* **2009**, *150*, 1687–1696. [[CrossRef](#)] [[PubMed](#)]
- Klessig, D.F.; Durner, J.; Noad, R.; Navarre, D.A.; Wendehenne, D.; Kumar, D.; Zhou, J.M.; Shah, J.; Zhang, S.; Kachroo, P.; et al. Nitric oxide and salicylic acid signaling in plant defense. *Proc. Natl. Acad. Sci. USA* **2000**, *97*, 8849–8855. [[CrossRef](#)] [[PubMed](#)]

23. Sánchez-Sanuy, F.; Cuadra, R.M.; Okada, K.; Sacchi, G.A.; Campo, S.; San Segundo, B. Iron treatment induces defense responses and disease resistance against *Magnaporthe oryzae* in rice. *bioRxiv* **2021**. [[CrossRef](#)]
24. Seutter von Loetzen, C.; Hoffmann, T.; Hartl, M.J.; Schweimer, K.; Schwab, W.; Rösch, P.; Hartl-Spiegelhauer, O. Secret of the major birch pollen allergen Bet v 1: Identification of the physiological ligand. *Biochem. J.* **2014**, *457*, 379–390. [[CrossRef](#)] [[PubMed](#)]
25. Ren, J.; Meng, S.; Lekka, C.E.; Kaxiras, E. Complexation of Flavonoids with Iron: Structure and Optical Signatures. *J. Phys. Chem. B* **2008**, *112*, 1845–1850. [[CrossRef](#)]
26. Morel, I.; Lescoat, G.; Cogrel, P.; Sergent, O.; Padeloup, N.; Brissot, P.; Cillard, P.; Cillard, J. Antioxidant and iron-chelating activities of the flavonoids catechin, quercetin and diosmetin on iron-loaded rat hepatocyte cultures. *Biochem. Pharmacol.* **1993**, *45*, 13–19. [[CrossRef](#)]
27. Kofler, S.; Asam, C.; Eckhard, U.; Wallner, M.; Ferreira, F.; Brandstetter, H. Crystallographically Mapped Ligand Binding Differs in High and Low IgE Binding Isoforms of Birch Pollen Allergen Bet v 1. *J. Mol. Biol.* **2012**, *422*, 109–123. [[CrossRef](#)]
28. Worda, J.M.; Lovell, S.; Richardson, J.; Richardson, D.C. Asparagine and glutamine: Using hydrogen atom contacts in the choice of side-chain amide orientation. *J. Mol. Biol.* **1999**, *285*, 1735–1747. [[CrossRef](#)]
29. Morris, G.M.; Huey, R.; Lindstrom, W.; Sanner, M.F.; Belew, R.K.; Goodsell, D.S.; Olson, A.J. AutoDock4 and AutoDockTools4: Automated docking with selective receptor flexibility. *J. Comput. Chem.* **2009**, *30*, 2785–2791. [[CrossRef](#)]
30. Trott, O.; Olson, A.J. AutoDock Vina: Improving the speed and accuracy of docking with a new scoring function, efficient optimization, and multithreading. *J. Comput. Chem.* **2010**, *31*, 455–461. [[CrossRef](#)]
31. Eberhardt, J.; Santos-Martins, D.; Tillack, A.F.; Forli, S. AutoDock Vina 1.2.0: New Docking Methods, Expanded Force Field, and Python Bindings. *J. Chem. Inf. Model.* **2021**, *61*, 3891–3898. [[CrossRef](#)] [[PubMed](#)]
32. Carson, M. Ribbons. *Methods Enzymol.* **1997**, *277*, 493–505. [[CrossRef](#)] [[PubMed](#)]
33. Pettersen, E.F.; Goddard, T.D.; Huang, C.C.; Couch, G.S.; Greenblatt, D.M.; Meng, E.C.; Ferrin, T.E. UCSF Chimera?A visualization system for exploratory research and analysis. *J. Comput. Chem.* **2004**, *25*, 1605–1612. [[CrossRef](#)] [[PubMed](#)]
34. Guhsl, E.E.; Hofstetter, G.; Hemmer, W.; Ebner, C.; Vieths, S.; Vogel, L.; Breiteneder, H.; Radauer, C. Vig r 6, the cytokinin-specific binding protein from mung bean (*Vigna radiata*) sprouts, cross-reacts with Bet v 1-related allergens and binds IgE from birch pollen allergic patients' sera. *Mol. Nutr. Food Res.* **2014**, *58*, 625–634. [[CrossRef](#)]
35. Erel, O. A novel automated direct measurement method for total antioxidant capacity using a new generation, more stable ABTS radical cation. *Clin. Biochem.* **2004**, *37*, 277–285. [[CrossRef](#)]
36. Miller, N.J.; Rice-Evans, C.; Davies, M.J.; Gopinathan, V.; Milner, A. A Novel Method for Measuring Antioxidant Capacity and its Application to Monitoring the Antioxidant Status in Premature Neonates. *Clin. Sci.* **1993**, *84*, 407–412. [[CrossRef](#)]
37. Petje, L.; Jensen, S.A.; Szikora, S.; Sulzbacher, M.; Bartosik, T.; Pjevac, P.; Hausmann, B.; Hufnagl, K.; Untersmayr, E.; Fischer, L.; et al. Functional iron-deficiency in women with allergic rhinitis is associated with symptoms after nasal provocation and lack of iron-sequestering microbes. *Allergy* **2021**, *76*, 2882–2886. [[CrossRef](#)]
38. Bartosik, T.; Jensen, S.A.; Afify, S.M.; Bianchini, R.; Hufnagl, K.; Hofstetter, G.; Berger, M.; Bastl, M.; Berger, U.; Rivelles, E.; et al. Ameliorating Atopy by Compensating Micronutritional Deficiencies in Immune Cells: A Double-Blind Placebo-Controlled Pilot Study. *J. Allergy Clin. Immunol. Pract.* **2022**, *10*, 1889–1902.e9. [[CrossRef](#)]
39. Folkerts, J.; Redegeld, F.; Folkerts, G.; Blokhuis, B.; van den Berg, M.P.; de Bruijn, M.J.; van IJcken, W.F.; Junt, T.; Tam, S.Y.; Galli, S.J.; et al. Butyrate inhibits human mast cell activation via epigenetic regulation of FcεpsilonRI-mediated signaling. *Allergy* **2020**, *75*, 1966–1978. [[CrossRef](#)]
40. Afify, S.M.; Regner, A.; Pacios, L.F.; Blokhuis, B.R.; Jensen, S.A.; Redegeld, F.A.; Pali-Schöll, I.; Hufnagl, K.; Bianchini, R.; Guethoff, S.; et al. Micronutritional supplementation with a holoBLG-based FSMP (food for special medical purposes)-lozenge alleviates allergic symptoms in BALB/c mice: Imitating the protective farm effect. *Clin. Exp. Allergy* **2022**, *52*, 426–441. [[CrossRef](#)]
41. Roth-Walter, F.; Afify, S.M.; Pacios, L.F.; Blokhuis, B.R.; Redegeld, F.; Regner, A.; Petje, L.M.; Fiocchi, A.; Untersmayr, E.; Dvorak, Z.; et al. Cow's milk protein beta-lactoglobulin confers resilience against allergy by targeting complexed iron into immune cells. *J. Allergy Clin. Immunol.* **2021**, *147*, 321–334.e4. [[CrossRef](#)] [[PubMed](#)]
42. Luscher, A.; Gasser, V.; Bumann, D.; Mislin, G.L.; Schalk, I.J.; Köhler, T. Plant-Derived Catechols Are Substrates of TonB-Dependent Transporters and Sensitize *Pseudomonas aeruginosa* to Siderophore-Drug Conjugates. *mBio* **2022**, *13*, e0149822. [[CrossRef](#)] [[PubMed](#)]
43. Roth-Walter, F. Iron-Deficiency in Atopic Diseases: Innate Immune Priming by Allergens and Siderophores. *Front. Allergy* **2022**, *3*, 859922. [[CrossRef](#)] [[PubMed](#)]
44. Gieras, A.; Cejka, P.; Blatt, K.; Focke-Tejkl, M.; Linhart, B.; Flicker, S.; Stoecklinger, A.; Marth, K.; Drescher, A.; Thalhamer, J.; et al. Mapping of Conformational IgE Epitopes with Peptide-Specific Monoclonal Antibodies Reveals Simultaneous Binding of Different IgE Antibodies to a Surface Patch on the Major Birch Pollen Allergen, Bet v 1. *J. Immunol.* **2011**, *186*, 5333–5344. [[CrossRef](#)] [[PubMed](#)]
45. Novotna, A.; Petr, P.; Dvorak, Z. Novel Stably Transfected Gene Reporter Human Hepatoma Cell Line for Assessment of Aryl Hydrocarbon Receptor Transcriptional Activity: Construction and Characterization. *Environ. Sci. Technol.* **2011**, *45*, 10133–10139. [[CrossRef](#)]
46. Mengos, A.E.; Gastineau, D.A.; Gustafson, M.P. The CD14(+)/HLA-DR(lo/neg) Monocyte: An Immunosuppressive Phenotype That Restrains Responses to Cancer Immunotherapy. *Front. Immunol.* **2019**, *10*, 1147. [[CrossRef](#)]
47. Wasuwanich, P.; Fan, G.; Burke, B.; Furst, A.L. Metal-phenolic networks as tuneable spore coat mimetics. *J. Mater. Chem. B* **2022**, *10*, 7600–7606. [[CrossRef](#)]

48. Khan, I.H.; Javaid, A. Biocontrol *Aspergillus* species together with plant biomass alter histochemical characteristics in diseased mungbean plants. *Microsc. Res. Tech.* **2022**, *85*, 2953–2964. [[CrossRef](#)]
49. Afify, S.M.; Pali-Schöll, I.; Hufnagl, K.; Hofstetter, G.; El-Bassuoni, M.A.-R.; Roth-Walter, F.; Jensen-Jarolim, E. Bovine Holo-Beta-Lactoglobulin Cross-Protects Against Pollen Allergies in an Innate Manner in BALB/c Mice: Potential Model for the Farm Effect. *Front. Immunol.* **2021**, *12*, 611474. [[CrossRef](#)]
50. Bergmann, K.C.; Raab, J.; Krause, L.; Becker, S.; Kugler, S.; Zuberbier, T.; Roth-Walter, F.; Jensen-Jarolim, E.; Kramer, M.F.; Graessel, A. Long-term benefits of targeted micronutrition with the holoBLG lozenge in house dust mite allergic patients. *Allergo J. Int.* **2022**, (*accepted*).
51. Bergmann, K.-C.; Graessel, A.; Raab, J.; Banghard, W.; Krause, L.; Becker, S.; Kugler, S.; Zuberbier, T.; Ott, V.B.; Kramer, M.F.; et al. Targeted micronutrition via holo-BLG based on the farm effect in house dust mite allergic rhinoconjunctivitis patients—First evaluation in a standardized allergen exposure chamber. *Allergo J. Int.* **2021**, *30*, 141–149. [[CrossRef](#)]
52. Lin, L.; Dai, Y.; Xia, Y. An overview of aryl hydrocarbon receptor ligands in the Last two decades (2002–2022): A medicinal chemistry perspective. *Eur. J. Med. Chem.* **2022**, *244*, 114845. [[CrossRef](#)] [[PubMed](#)]
53. Koch, S.; Stroisch, T.J.; Vorac, J.; Herrmann, N.; Leib, N.; Schnautz, S.; Kirins, H.; Förster, I.; Weighardt, H.; Bieber, T. AhR mediates an anti-inflammatory feedback mechanism in human Langerhans cells involving FcepsilonRI and IDO. *Allergy* **2017**, *72*, 1686–1693. [[CrossRef](#)] [[PubMed](#)]
54. Roth-Walter, F.; Bergmayr, C.; Meitz, S.; Buchleitner, S.; Stremnitzer, C.; Fazekas-Singer, J.; Moskovskich, A.; Müller, M.A.; Roth, G.A.; Manzano-Szalai, K.; et al. Janus-faced Acrolein prevents allergy but accelerates tumor growth by promoting immunoregulatory Foxp3+ cells: Mouse model for passive respiratory exposure. *Sci. Rep.* **2017**, *7*, 45067. [[CrossRef](#)] [[PubMed](#)]
55. Gandhi, R.; Kumar, D.; Burns, E.J.; Nadeau, M.; Dake, B.; Laroni, A.; Kozoriz, D.; Weiner, H.L.; Quintana, F.J. Activation of the aryl hydrocarbon receptor induces human type 1 regulatory T cell-like and Foxp3+ regulatory T cells. *Nat. Immunol.* **2010**, *11*, 846–853. [[CrossRef](#)] [[PubMed](#)]
56. Negishi, T.; Kato, Y.; Ooneda, O.; Mimura, J.; Takada, T.; Mochizuki, H.; Yamamoto, M.; Fujii-Kuriyama, Y.; Furusako, S. Effects of aryl hydrocarbon receptor signaling on the modulation of TH1/TH2 balance. *J. Immunol.* **2005**, *175*, 7348–7356. [[CrossRef](#)]
57. Aguilera-Montilla, N.; Chamorro, S.; Nieto, C.; Sánchez-Cabo, F.; Dopazo, A.; Fernández-Salguero, P.M.; Rodríguez-Fernández, J.L.; Pello, O.M.; Andrés, V.; Cuenda, A.; et al. Aryl hydrocarbon receptor contributes to the MEK/ERK-dependent maintenance of the immature state of human dendritic cells. *Blood* **2013**, *121*, e108–e117. [[CrossRef](#)]
58. Agoro, R.; Taleb, M.; Quesniaux, V.F.J.; Mura, C. Cell iron status influences macrophage polarization. *PLoS ONE* **2018**, *13*, e0196921. [[CrossRef](#)]
59. Carrasco-Marín, E.; Alvarez-Domínguez, C.; Lopez-Mato, P.; Martínez-Palencia, R.; Leyva-Cobian, F.; Carrasco-Marín, E. Iron Salts and Iron-Containing Porphyrins Block Presentation of Protein Antigens by Macrophages to MHC Class II-Restricted T Cells. *Cell Immunol.* **1996**, *171*, 173–185. [[CrossRef](#)]
60. Leung, S.; Holbrook, A.; King, B.; Lu, H.-T.; Evans, V.; Miyamoto, N.; Mallari, C.; Harvey, S.; Davey, D.; Ho, E.; et al. Differential Inhibition of Inducible T Cell Cytokine Secretion by Potent Iron Chelators. *J. Biomol. Screensupp.* **2005**, *10*, 157–167. [[CrossRef](#)]
61. Jason, J.; Archibald, L.K.; Nwyanwu, O.C.; Bell, M.; Jensen, R.J.; Gunter, E.; Buchanan, I.; Larned, J.; Kazembe, P.N.; Dobbie, H.; et al. The effects of iron deficiency on lymphocyte cytokine production and activation: Preservation of hepatic iron but not at all cost. *Clin. Exp. Immunol.* **2001**, *126*, 466–473. [[CrossRef](#)]
62. Thorson, J.A.; Smith, K.M.; Gomez, F.; Naumann, P.W.; Kemp, J.D. Role of iron in T cell activation: Th1 clones differ from TH2 clones in their sensitivity to inhibition of DNA synthesis caused by IGG mabs against the transferrin receptor and the iron chelator deferoxamine. *Cell. Immunol.* **1991**, *134*, 126–137. [[CrossRef](#)] [[PubMed](#)]
63. Drury, K.E.; Schaeffer, M.; Silverberg, J.I. Association Between Atopic Disease and Anemia in US Children. *JAMA Pediatr.* **2016**, *170*, 29–34. [[CrossRef](#)] [[PubMed](#)]
64. Rhew, K.; Brown, J.D.; Oh, J.M. Atopic Disease and Anemia in Korean Patients: Cross-Sectional Study with Propensity Score Analysis. *Int. J. Environ. Res. Public Health* **2020**, *17*, 1978. [[CrossRef](#)] [[PubMed](#)]
65. Rhew, K.; Oh, J.M. Association between atopic disease and anemia in pediatrics: A cross-sectional study. *BMC Pediatr.* **2019**, *19*, 455. [[CrossRef](#)]
66. Shaheen, S.O.; Gissler, M.; Devereux, G.; Erkkola, M.; Kinnunen, T.I.; Mcardle, H.; Sheikh, A.; Hemminki, E.; Nwaru, B.I. Maternal iron supplementation in pregnancy and asthma in the offspring: Follow-up of a randomised trial in Finland. *Eur. Respir. J.* **2020**, *55*, 1902335. [[CrossRef](#)]
67. Shaheen, S.O.; Macdonald-Wallis, C.; Lawlor, D.A.; Henderson, A.J. Haemoglobin concentrations in pregnancy and respiratory and allergic outcomes in childhood: Birth cohort study. *Clin. Exp. Allergy* **2017**, *47*, 1615–1624. [[CrossRef](#)]
68. Shaheen, S.; Newson, R.; Henderson, A.; Emmett, P.; Sherriff, A.; Cooke, M. The ALSPAC Study Team Umbilical cord trace elements and minerals and risk of early childhood wheezing and eczema. *Eur. Respir. J.* **2004**, *24*, 292–297. [[CrossRef](#)]
69. Nyakeriga, A.M.; Williams, T.N.; Marsh, K.; Wambua, S.; Perlmann, H.; Grandien, A.; Troye-Blomberg, M. Cytokine mRNA Expression and Iron Status in Children Living in a Malaria Endemic Area. *Scand. J. Immunol.* **2005**, *61*, 370–375. [[CrossRef](#)]
70. DeRosa, A.; Leftin, A. The Iron Curtain: Macrophages at the Interface of Systemic and Microenvironmental Iron Metabolism and Immune Response in Cancer. *Front. Immunol.* **2021**, *12*, 614294. [[CrossRef](#)]

71. Walter, P.B.; Knutson, M.D.; Paler-Martinez, A.; Lee, S.; Xu, Y.; Viteri, F.E.; Ames, B.N. Iron deficiency and iron excess damage mitochondria and mitochondrial DNA in rats. *Proc. Natl. Acad. Sci. USA* **2002**, *99*, 2264–2269. [[CrossRef](#)]
72. Barreto, L.R.; Barreto, T.; Melo, S.; Pungartnik, C.; Brendel, M. Sensitivity of Yeast Mutants Deficient in Mitochondrial or Vacuolar ABC Transporters to Pathogenesis-Related Protein TcPR-10 of *Theobroma cacao*. *Biology* **2018**, *7*, 35. [[CrossRef](#)] [[PubMed](#)]

Disclaimer/Publisher’s Note: The statements, opinions and data contained in all publications are solely those of the individual author(s) and contributor(s) and not of MDPI and/or the editor(s). MDPI and/or the editor(s) disclaim responsibility for any injury to people or property resulting from any ideas, methods, instructions or products referred to in the content.